

Energy Harvesting and Magnetic Field Sensing with Bidomain LiNbO_3 -Based Composites

N.A. Sobolev^{1,2}, A.V. Turutin², J.V. Vidal^{1,3}, I.V. Kubasov², A.M. Kislyuk², S.P. Kobeleva², D.A. Kiselev², A.S. Bykov², A.A. Temirov², R.N. Zhukov², M.D. Malinkovich², Y.N. Parkhomenko², A.L. Kholkin^{2,3}

¹ Department of Physics and I3N, University of Aveiro, 3810-193 Aveiro, Portugal

² National University of Science and Technology “MISIS”, 119049 Moscow, Russia

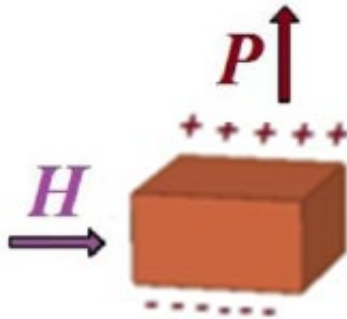
³ Department of Physics and CICECO, University of Aveiro, 3810-193 Aveiro, Portugal



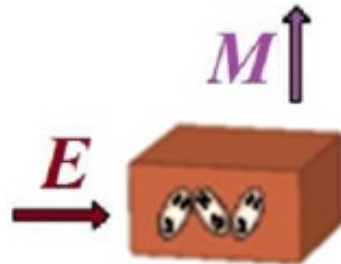
Introduction

The linear Magnetolectric (ME) effect

- Direct ME effect (ME_H):
- Converse ME effect (ME_E):

$$P_i = \alpha_{ij} H_j$$


- Induction of a polarization, \mathbf{P} , by an applied magnetic field, \mathbf{H} .

$$\mu_0 M_i = \alpha_{ij} E_j$$


- Induction of a magnetization, \mathbf{M} , by an applied electric field, \mathbf{E} .

* α_{ij} (s/m) - linear ME susceptibility tensor.

Introduction

ME composites

$$\text{ME}_H \text{ effect} = \frac{\text{Electrical}}{\text{Mechanical}} \times \frac{\text{Mechanical}}{\text{Magnetic}};$$

Piezoelectricity ↓

↙ Magnetostriction

$$\alpha_{ij} = k_c (\partial P_i / \partial H_j) = k_c (\partial P_i / \partial S_k) (\partial S_k / \partial H_j) = k_c d_{ik} q_{jk};$$

The figure of merit, **direct ME voltage coefficient** (α_{Eij}), is ca. proportional to the ratio between d and ϵ :

$$\alpha_{Eij} = \partial E_i / \partial H_j = \alpha_{ij} / \epsilon_{ij} \text{ (V/(cm}\cdot\text{Oe))}$$

Thus, alternatives to PZT and PMN-PT (which have a low Curie temperature, large hysteresis, creep effect, etc.) such as single-crystalline lead-free PEs can also exhibit **large α_{Eij} in composites**, as we have shown for the case of LiNbO₃ and GaPO₄

[JAP **114**, 044102 (2013), Vacuum **122**, 286 (2015)].

Introduction

Applications

- New sensors are needed for the detection of **low-frequency minute magnetic field (H) variations** in applications ranging from biomagnetics to magnetic anomaly detectors;
- **PE bimorphs** (PE plates with opposing polarizations) with large α_{Eij} at low frequencies have been singled out [[J. Zhai et al., APL 88, 062510 \(2006\)](#)] as natural contenders for this applications.

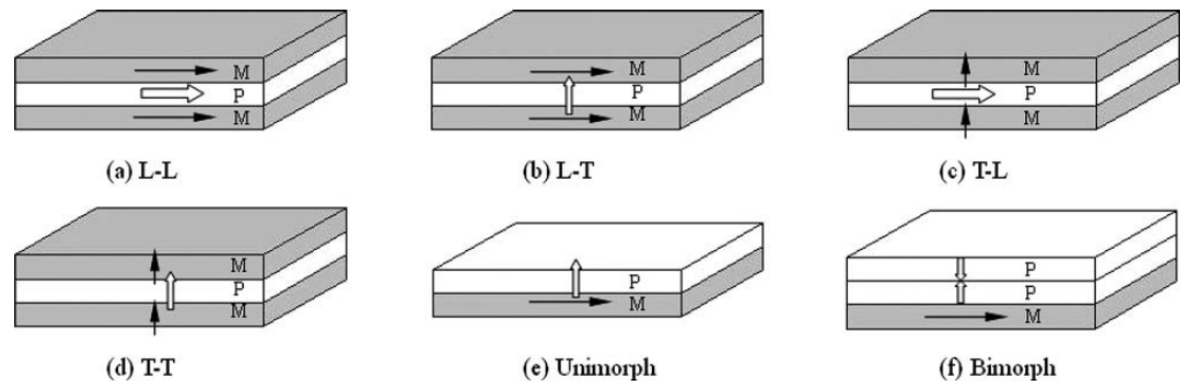
Piezoelectric bimorphs

- Usually obtained by gluing or sintering oppositely polarized plates together;
- Recently, **bidomains in single-crystals of LiNbO_3 and LiTaO_3** with strong linear bending deformations have been developed for applications in precision EM actuators.

Introduction

Figure: Various operation modes in ME laminates

[Z. Xing et al., JAP **106**, 024512 (2009)]



Asymmetric structures (bilayers) vs. Symmetric structures (trilayers):

- X Smaller ME effects at higher frequencies;
- ✓ Stronger ME effects at lower frequencies (bending modes);
- ✓ Partial rejection of thermal and vibrational noise.

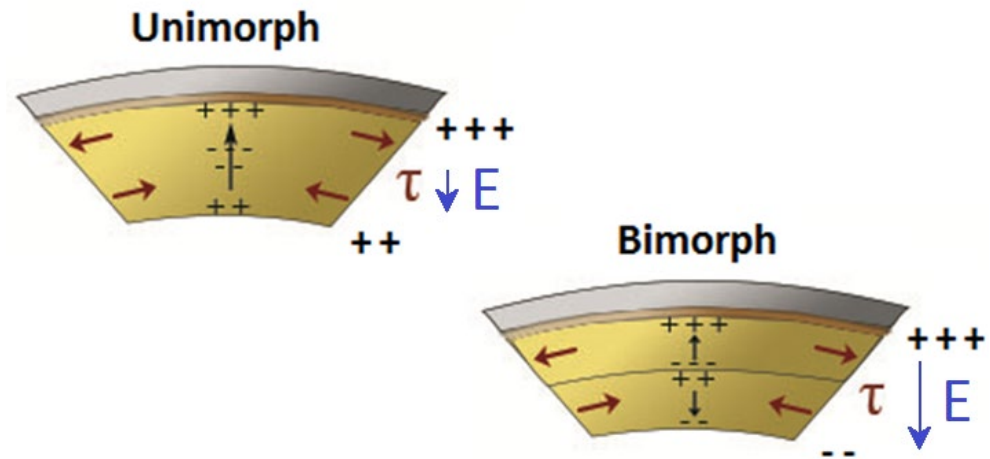


Figure: Stronger bending ME effect is expected in the bimorph vs. unimorph.

Introduction

We propose the use of bidomain LiNbO_3 single crystals for applications in sensitive, low-frequency and high-temperature magnetic field vector sensors.

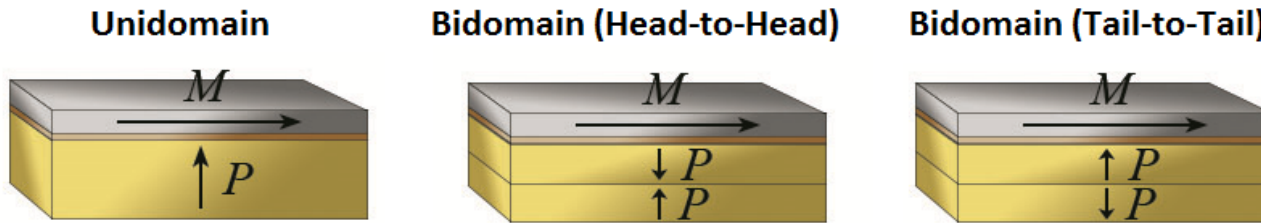


Figure: Types of ME bilayered composites studied in this work.



Figure: Optical microscopy image of the bidomain structure in a LN crystal.

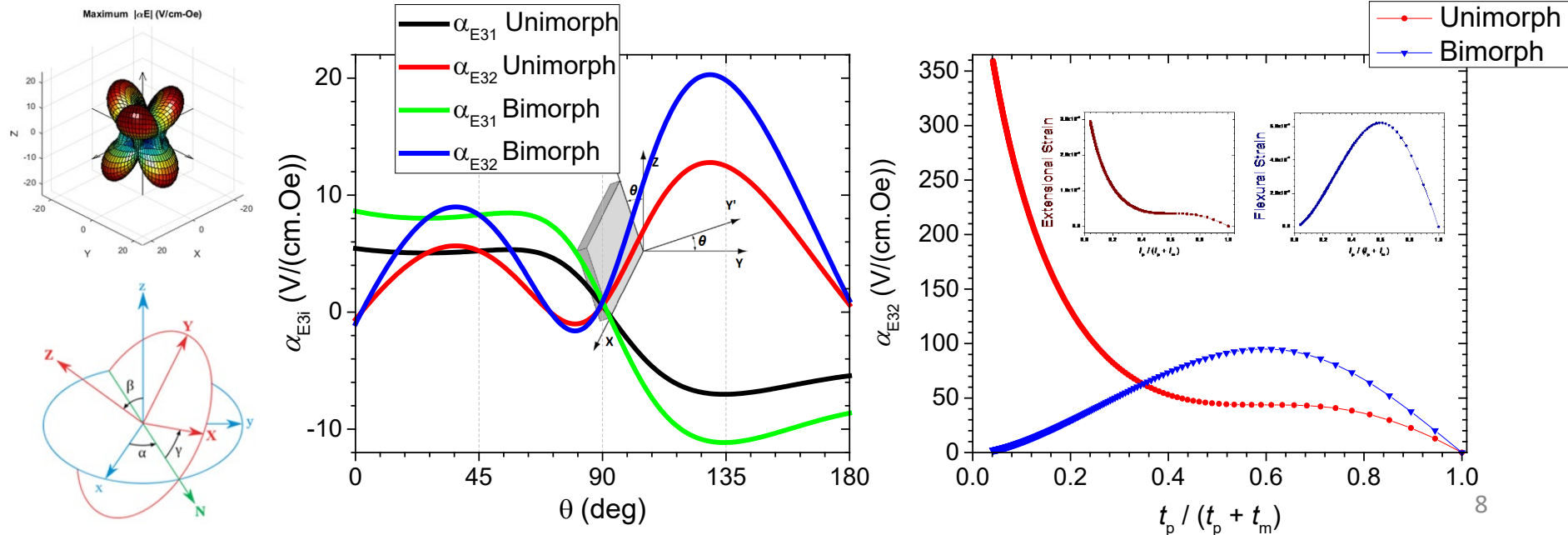
Preliminary calculations

➤ Maximum expected anisotropic ME coefficients were calculated by means of an averaging quasi-static method

Figure: Maximum transversal ME coefficients vs. cut angle in relation to the y crystalline axis.

- α_{E3a} is maximized in the y+127°-cut.

Figure: α_{E32} for the y+127°-cut crystal vs. thickness ratio of the PE phase.



Experimental

- Ferroelectric bidomain “head-to-head” (H-H) and “tail-to-tail” (T-T) structures were formed in $10 \times 10 \times 0.5 \text{ mm}^3$ commercial congruent single-crystalline $y+127^\circ$ -cut LiNbO_3 plates;
 - Two techniques were used:
 - **Stationary external light heating (SEH)** creating a temperature gradient throughout the plate thickness [A.S. Bykov et al., *Russ. Microelectron.* **43**, 536 (2014)];
 - **Directed diffusion annealing (DA)** of Li_2O in LiNbO_3 during high-temperature treatment [K. Nakamura et al., *APL* **50**, 1413 (1987)]
- Up to 5 commercial $29 \mu\text{m}$ thick foils of amorphous MS Metglas[®] alloy were bonded to one face of the plates using an epoxy resin to form the ME bilayered composites.

Experimental

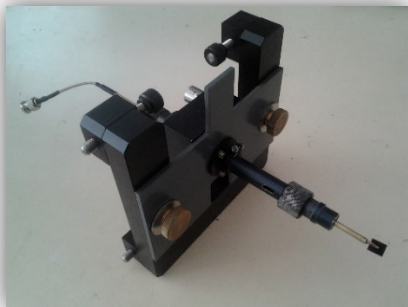
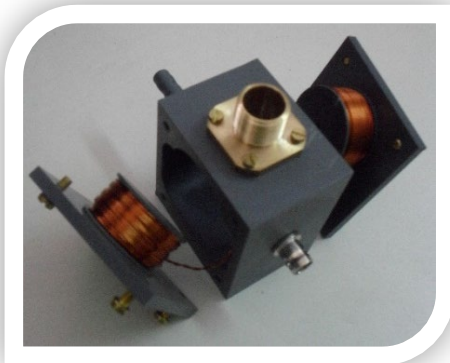
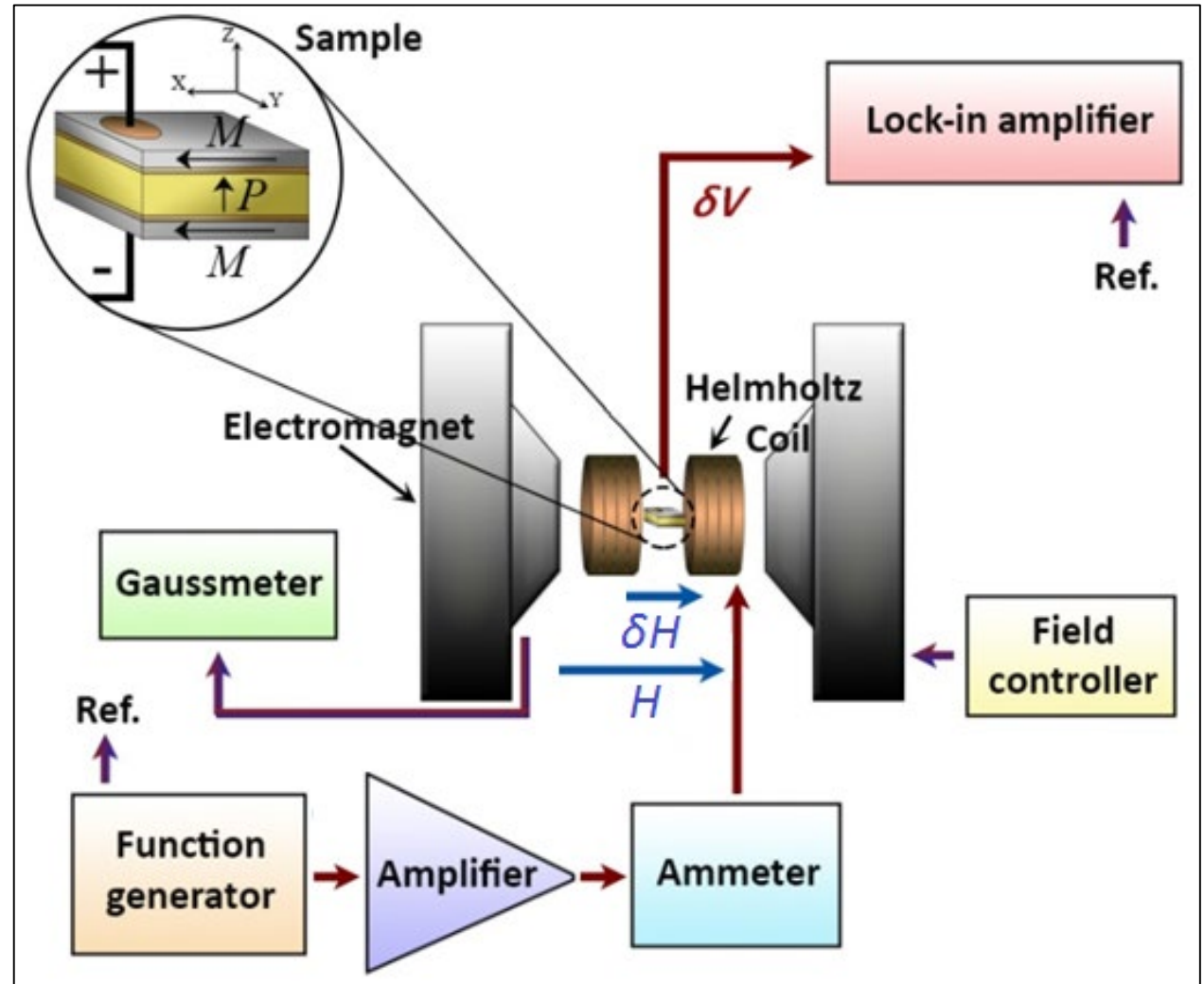
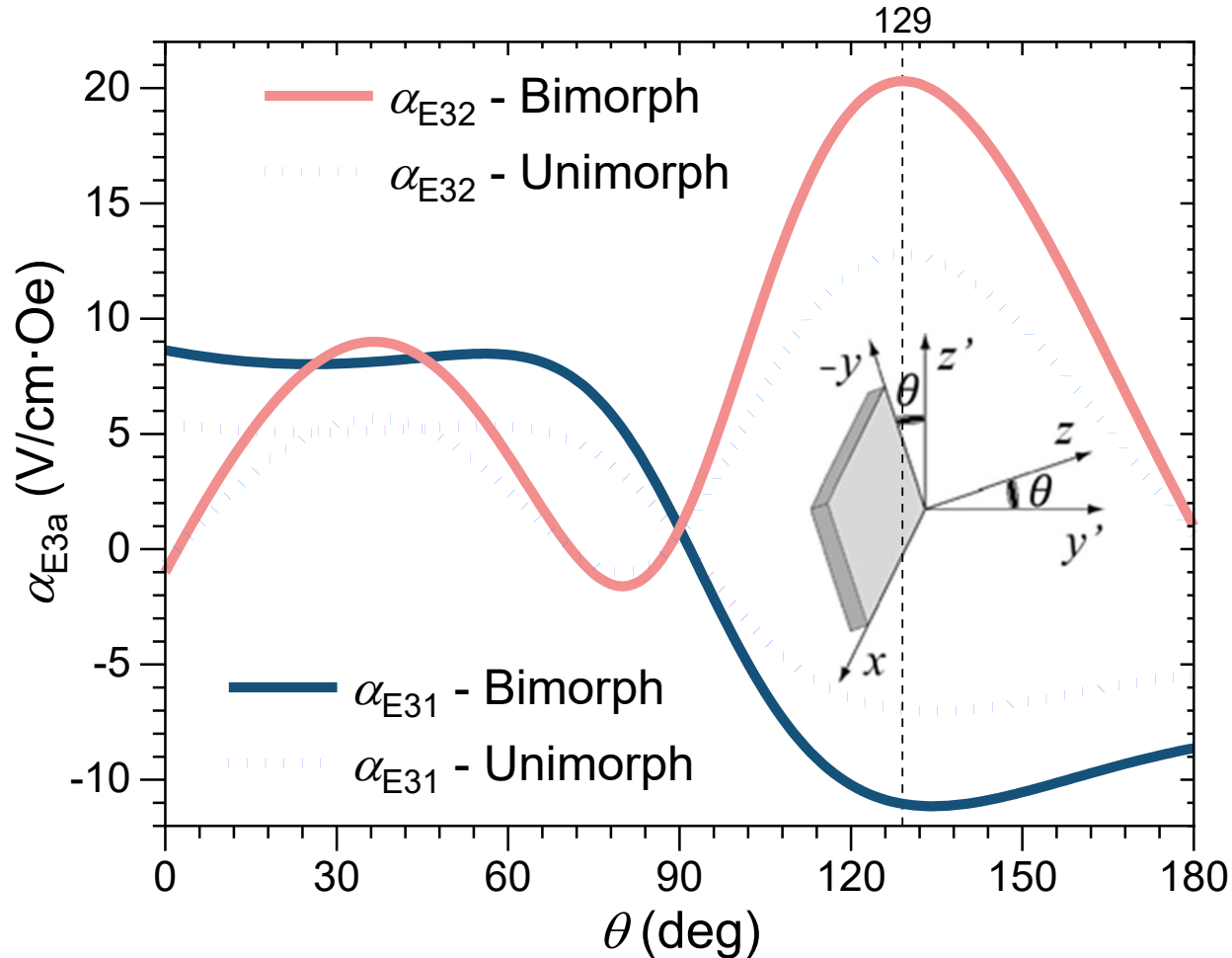


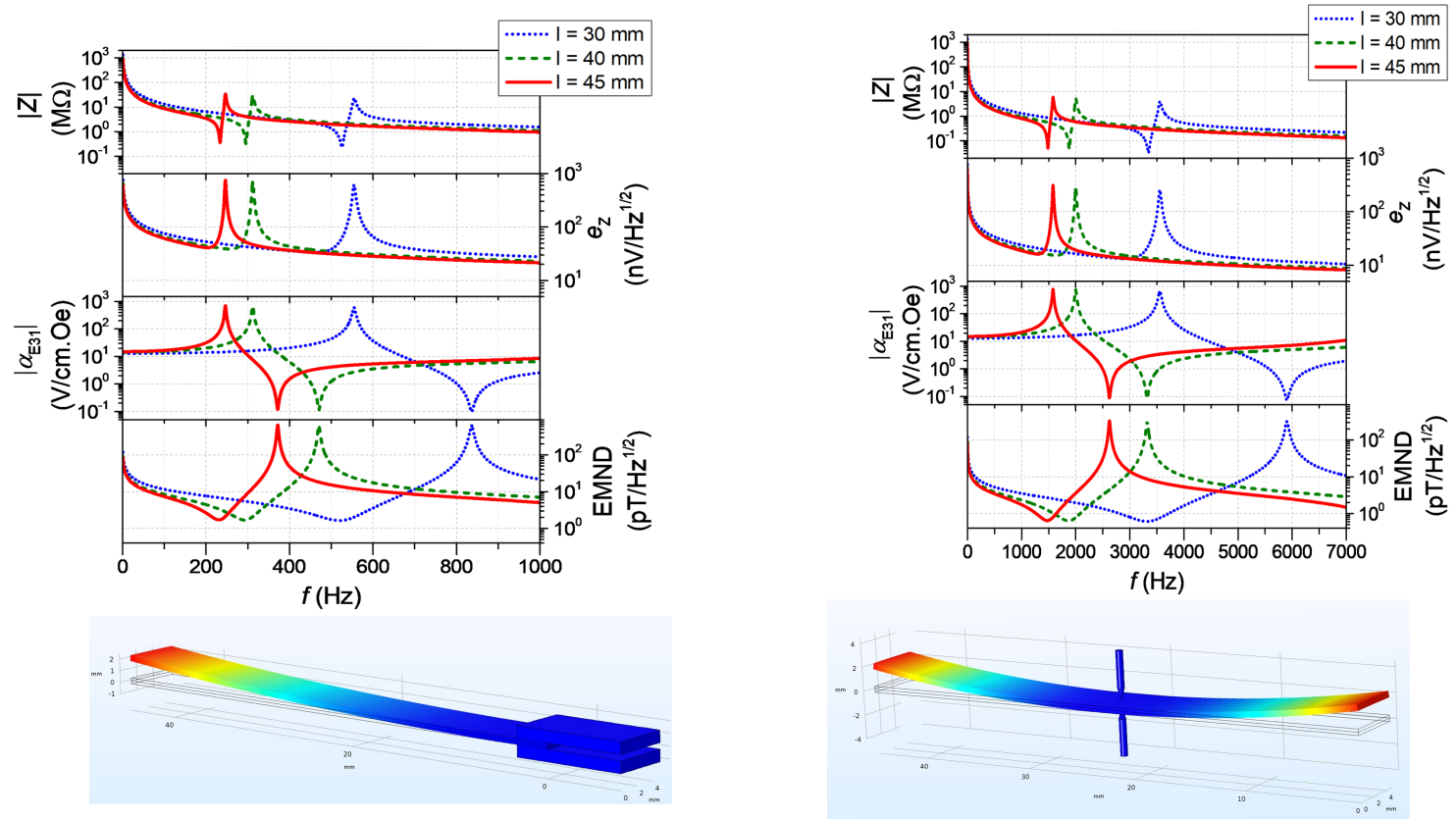
Figure: Experimental setup used in the ME measurements ($\alpha_{Eij} = \delta V_i / t \cdot \delta H_j$).

Calculations



ME coefficients calculated for two perpendicular magnetic field directions in the sample plane in composites with a monodomain and bidomain LN crystal as a function of the cut angle θ .

Calculations



Top: Calculated values of the absolute impedance ($|Z|$), thermal noise (e_z), ME coefficient ($|\alpha_{E32}|$) and the equivalent magnetic noise density (EMND) vs. frequency for the cantilever-type and free bar-type fixation.

Bottom: FE modeling of the bending deformation of a $y+127^\circ$ cut LN crystal for the two fixation types.

Quasi-static ME effect

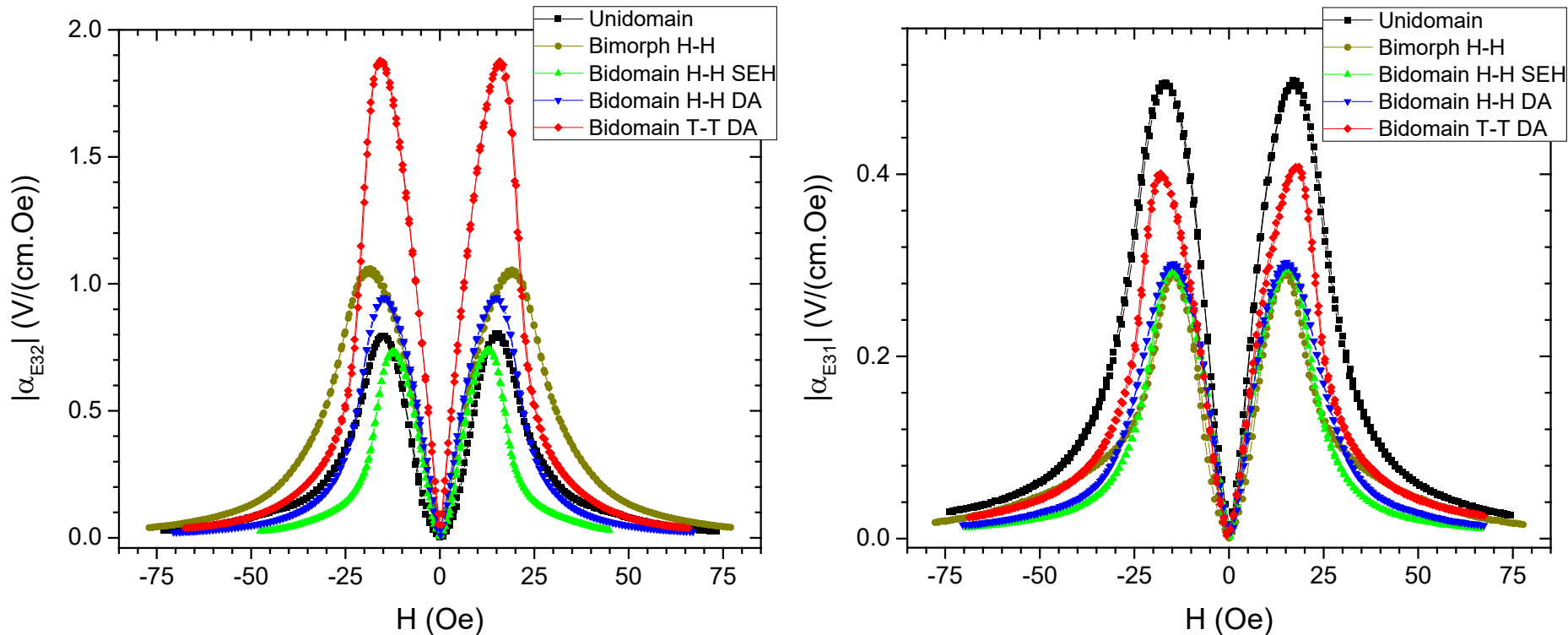


Figure: Transversal $|\alpha_{E3a}|$ vs. bias field (H) for the $y+127^\circ$ -cut LN bidomain and unidomain samples with a single layer of metglas (@ 1 kHz).

Quasi-static regime: Conclusions

- (i) Large anisotropy of the in-plane ME coefficients α_{E31} and α_{E32} ;
- (ii) Transversal ME effect α_{E32} obtained in a bidomain T-T sample produced by DA is twice as large as in the other samples;
- (ii) Theoretically obtained coefficients reasonably agree with the ones observed in the bidomain T-T DA and unidomain samples.

Impedance spectra

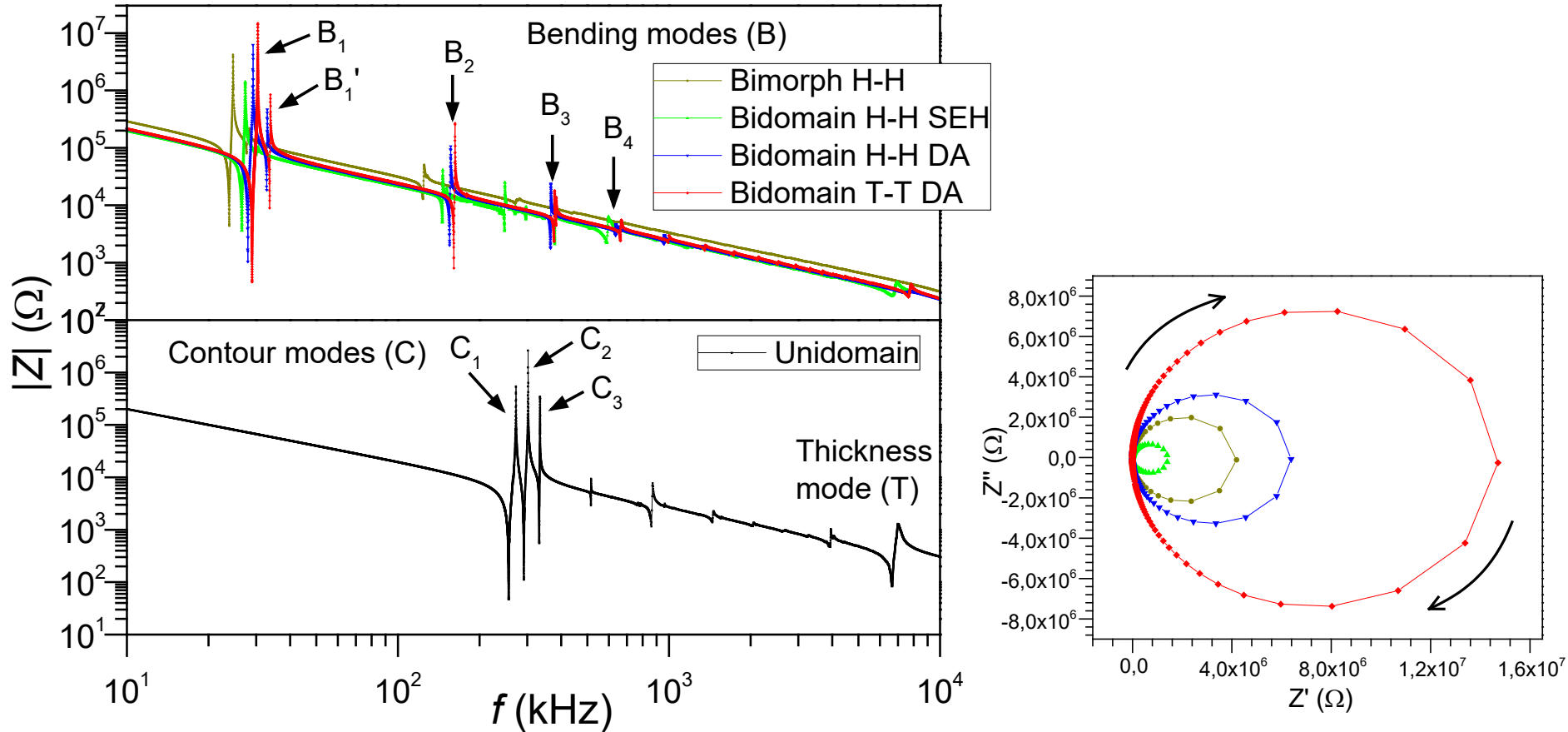


Figure: $|Z|$ vs. frequency (f) and Nyquist plots for the $y+127^\circ$ -cut LN bidomain and unidomain crystals.

Impedance: Conclusions

- (i)** Fundamental low-frequency (ca. 30 kHz) resonant electromechanical bending modes (B) appear in the bidomain crystals, while higher-frequency (ca. 300 kHz) in-plane contour extensional modes (C) are suppressed;
- (ii)** The opposite is verified in the unidomain crystals;
- (iii)** The amplitudes of the impedance peaks are larger in the bidomain crystals fabricated by DA relative to those produced by SEH;
- iv)** They are also larger as compared to the bimorph H-H crystals produced by simply bonding two crystals together with epoxy.

Resonant ME effect

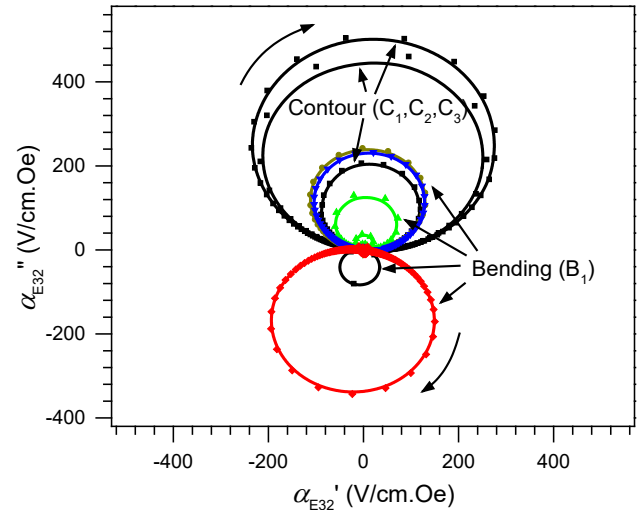
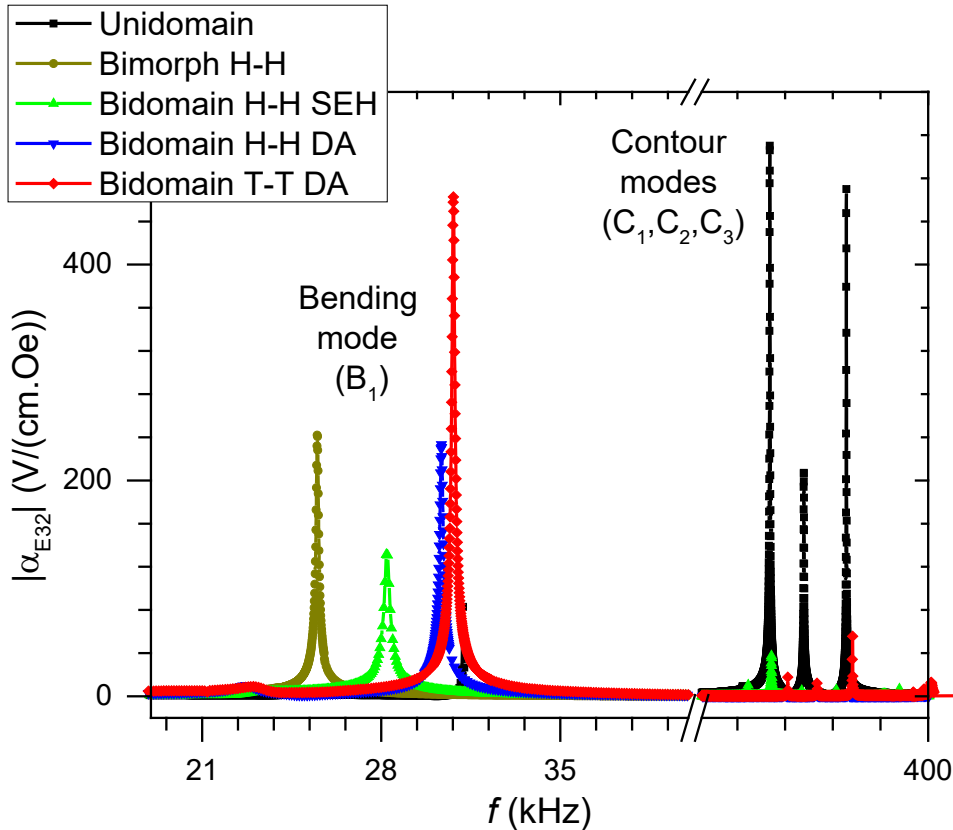


Figure: $|\alpha_{E32}|$ vs. frequency (f) and Nyquist plot of the samples with a single metglas layer in an optimal bias field of ca. 16 Oe.

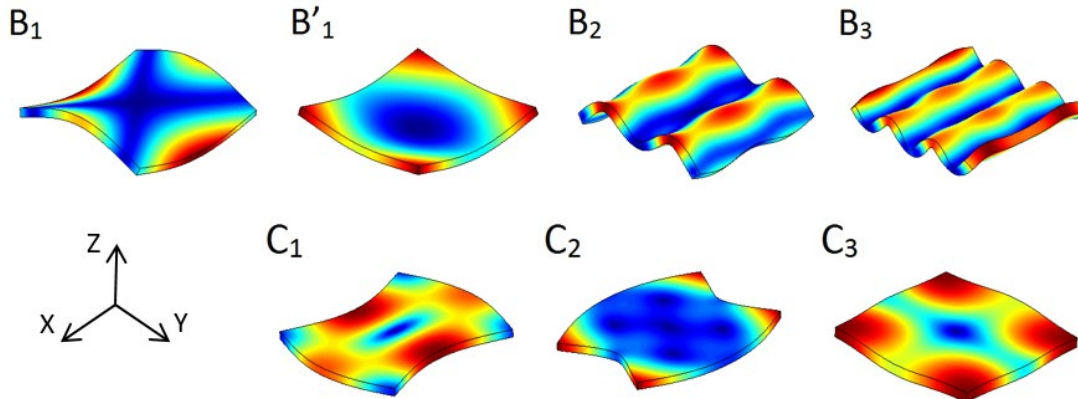


Figure: Different resonant modes as simulated by FEM.

Resonant regime: Conclusions

- (i) ME voltage coefficient is greatly enhanced under EM resonance conditions;
- (ii) ME voltage coefficient is nearly proportional to $i\omega Z$ close to the resonance, and therefore the ME resonant frequencies correspond to the antiresonant frequencies of Z ;
- (iii) Large ME effects of up to ≈ 500 V/(cm·Oe) were obtained @ 31 kHz in the Bidomain T-T $y+127^\circ$ -cut LNO sample fabricated by DA;
- (iv) In the other samples, the ME effects in the fundamental bending mode were up to: 242 V/(cm·Oe) in the bimorph H-H, 233 in the bidomain H-H DA, 131 in the bidomain H-H SEH and 83 in the unidomain.

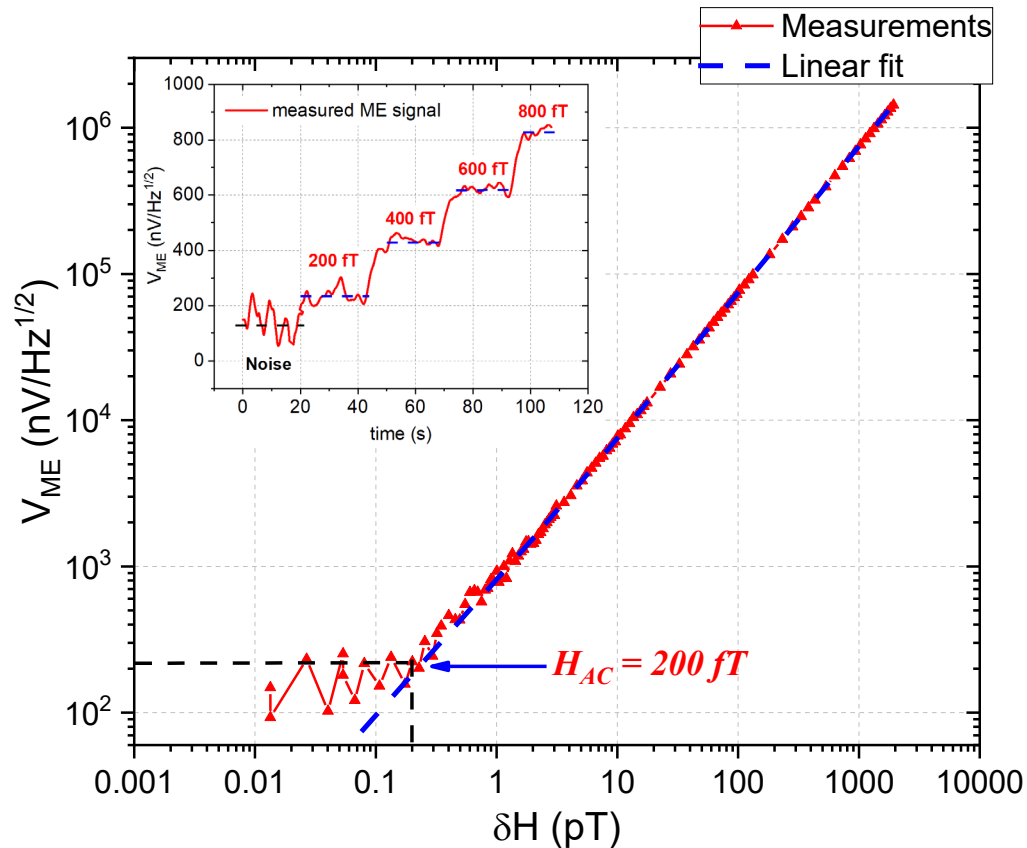
Resonant regime: Conclusions

(v) Strong contour modes were observed in the unidomain samples at higher frequencies (about 300 kHz) with α_{E32} of up to 504 V/(cm·Oe). In the bidomain samples the effect was much weaker (< 37 V/(cm·Oe));

(vi) The bending ME resonant effect is enhanced (larger ME coefficient and Q factor) in the T-T DA sample in comparison with the bimorph. It is approximately equivalent in both the H-H DA and bimorph samples and weaker in the H-H SEH sample;

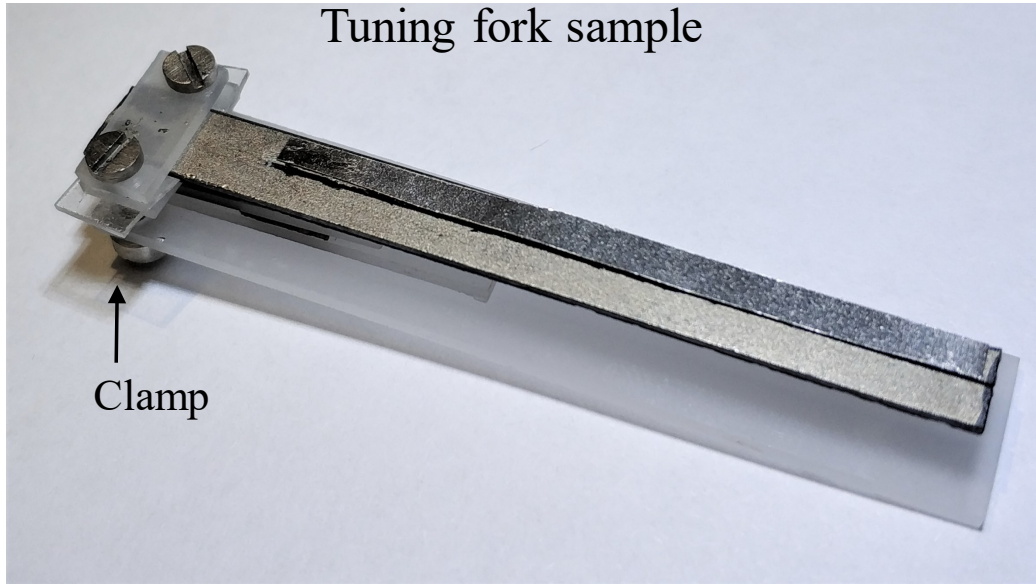
(vii) The PE T-T bimorphs produced by DA have a better quality which is mainly related to the smoothness of the non-piezoelectric transition polydomain area between the domains.

Noise measurements

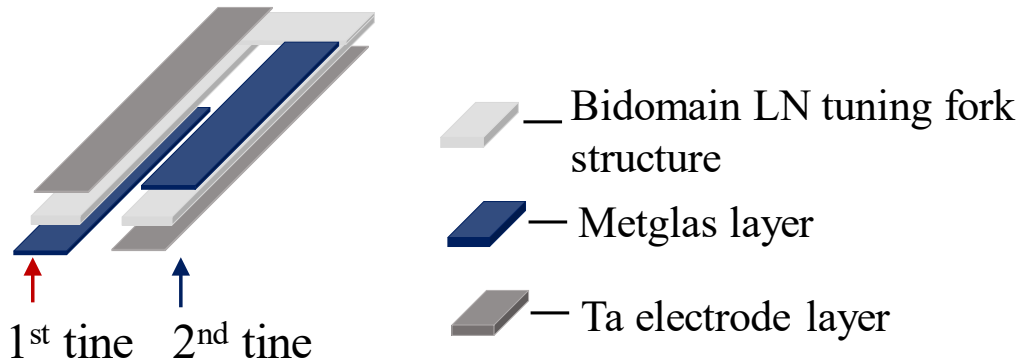


Magnetic field detection limit by a composite comprising a $y+140^\circ$ -cut LN crystal at a modulation frequency of 6862 Hz with an applied constant field of 5 Oe. Measurements were made without shielding from external noises. The ME coefficient in such samples achieves $1704 \text{ V} \cdot (\text{cm} \cdot \text{Oe})^{-1}$.

Tuning fork



Layer scheme

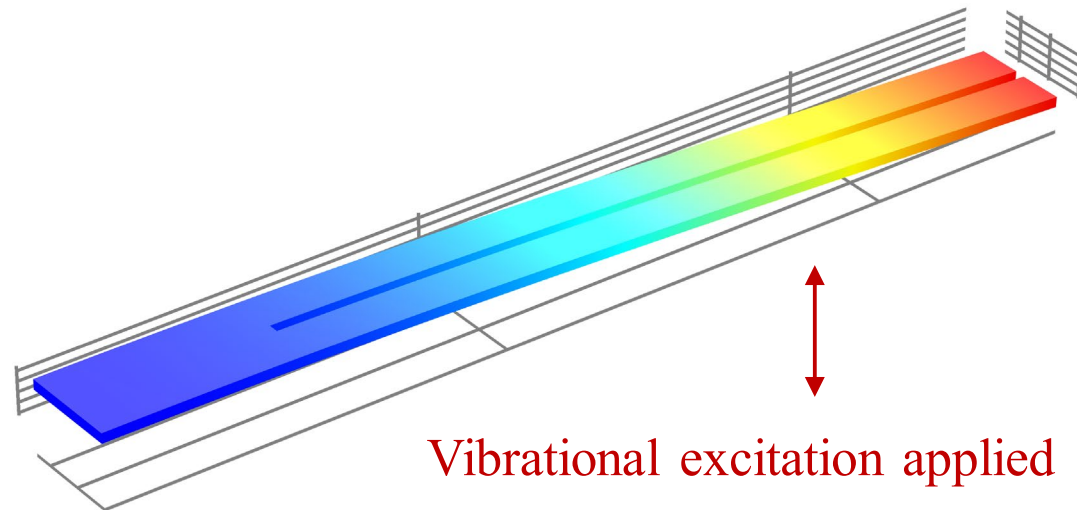
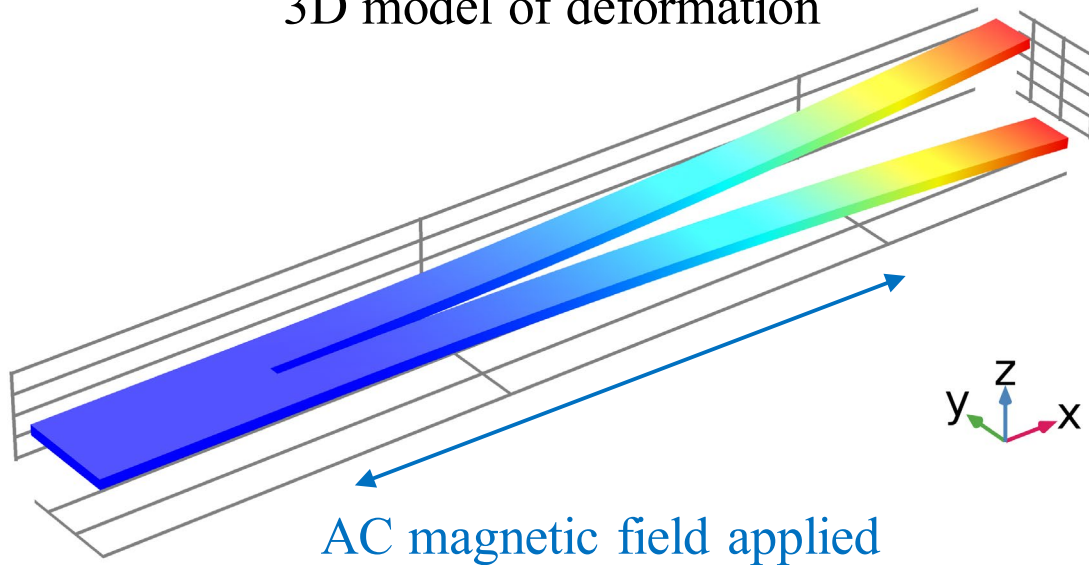


The maximum sensitivity of a ME field sensor is achieved at the EM resonance of the composite, but at these conditions the sensors are very susceptible also to acoustical and other external noise sources.

To suppress the influence of external noises, we proposed a composite in form of a **tuning fork** made of a single $y+128^\circ$ -cut LN crystal with an asymmetrical arrangement of metglas layers.

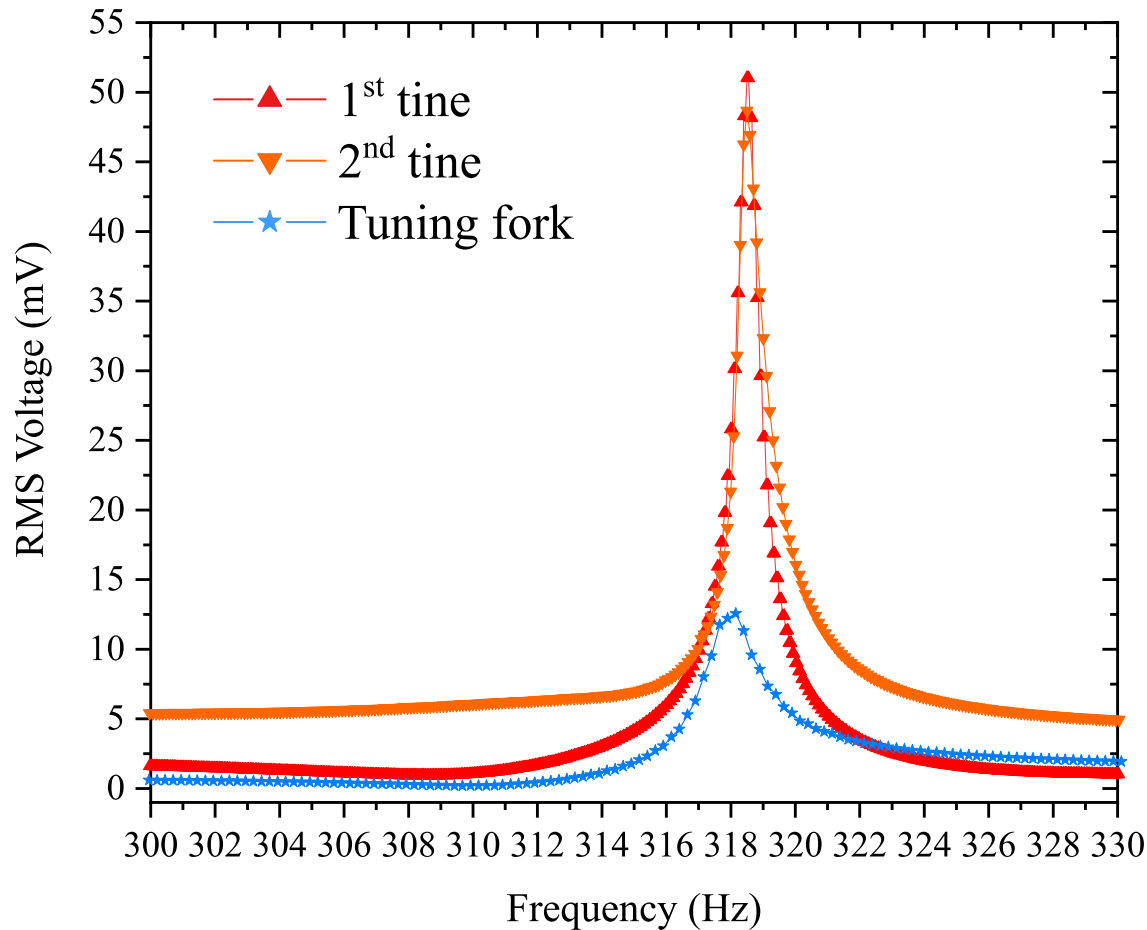
Tuning fork

3D model of deformation



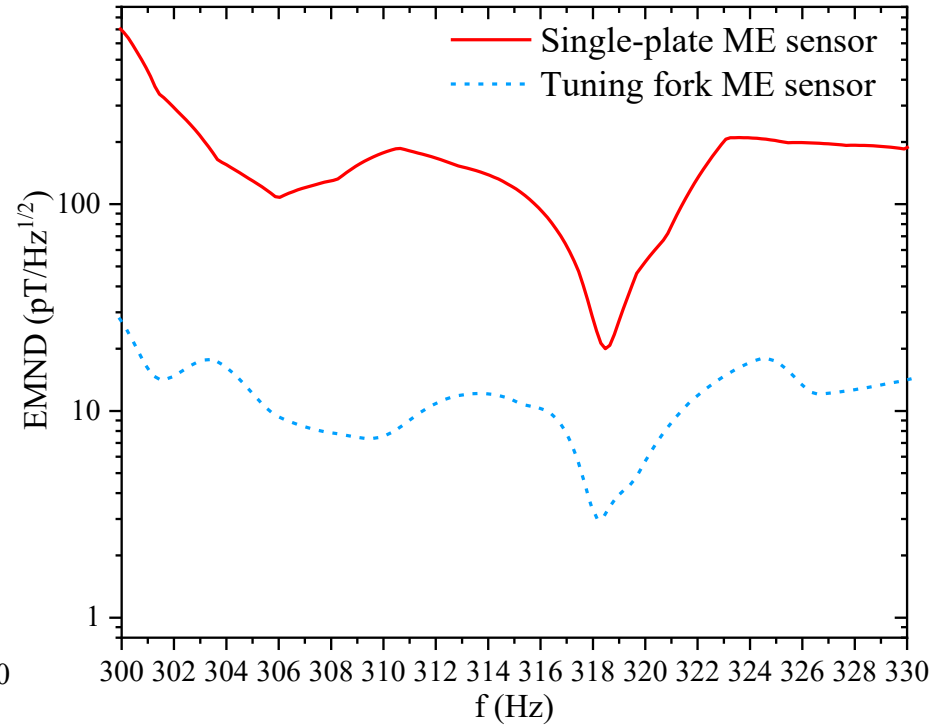
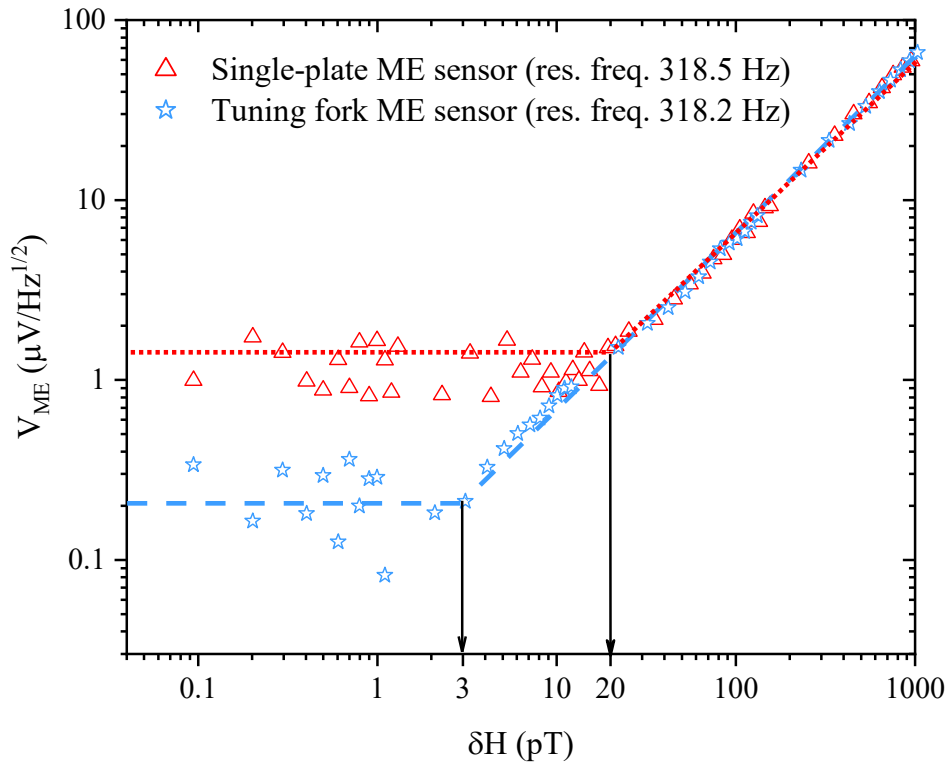
3D model of the deformation of a ME tuning fork when a magnetic field and a mechanical vibration are applied.

Tuning fork



Output voltage of a tuning fork ME sensor vs. frequency of the vibrational excitation in the vicinity of the bending resonance.

Tuning fork



(a) Linear dependence of the ME voltage on the applied AC magnetic fields at the resonance frequency of the 1st line of the ME sample (318.5 Hz) and of the tuning fork (318.2 Hz) in an optimum DC magnetic field. Dashed lines show the noise floor which determines the detection limit of the magnetic field. **(b)** Spectral noise density vs. frequency.

Noise: Conclusions

- (i) With a $y+128^\circ$ -cut LN crystal at EM antiresonance conditions ($f = 30.8$ kHz, maximum signal output) the best sensitivity of 524 fT/Hz^{1/2} (SNS = 1) was obtained.
- (ii) The use of a $y+140^\circ$ -cut LN crystal permitted to achieve an equivalent magnetic noise density of 92 fT/Hz^{1/2} at an antiresonance frequency of 6862 Hz.
- (iii) Using a composite in form of a cantilever with a small mass at the free end permits lowering the resonance frequency as well as achieving a ME coefficient of >500 V/(cm·Oe) at frequencies <100 Hz. Shielding against external noises should lead to detectivities of <2 pT/Hz^{1/2}.

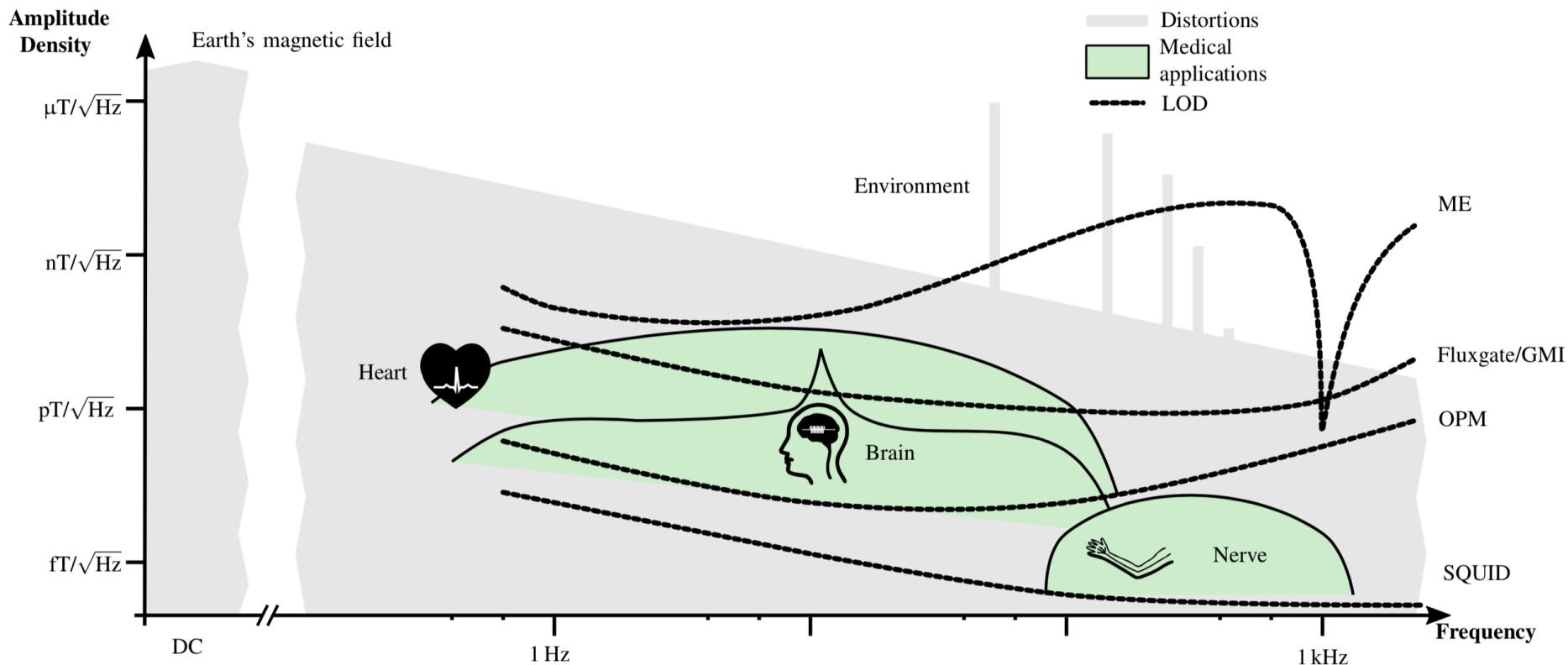
Noise: Conclusions

(iv) A significant suppression of vibrational noises was achieved by using a tuning fork-shaped ME composite with asymmetrical arrangement of metglas layers.

Off resonance, the noise suppression varied between 7 and 25 times as compared to a single tine.

At resonance the improvement amounted to a factor of 6.7.

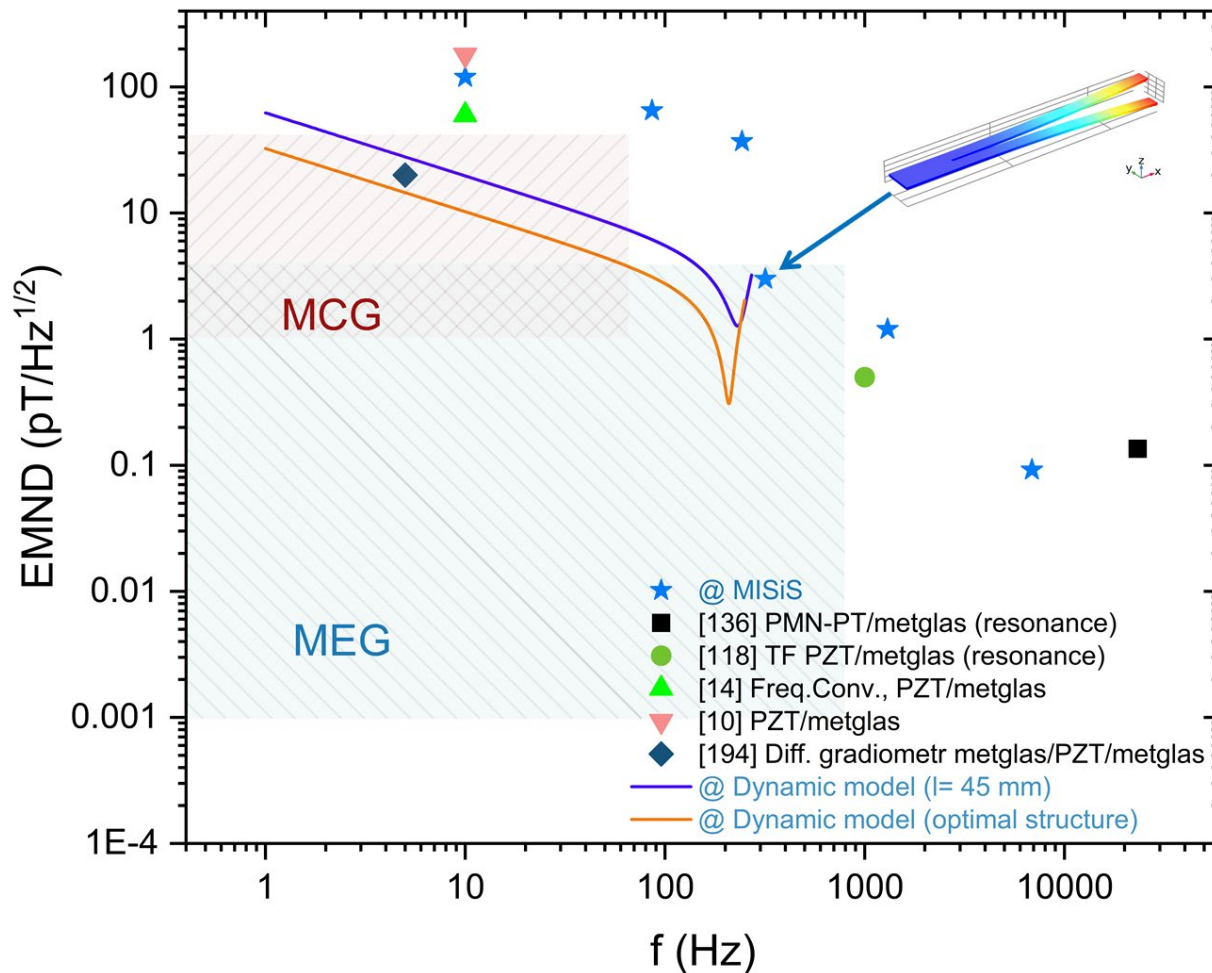
Magnetic field sensors



Comparison of typical magnetic field amplitudes for various medical applications, noise sources and detection limits of several sensor types

[J. Reermann et al., IEEE Sensors J. (2019)]

Magnetic field sensors



Comparison of the sensitivity to magnetic fields (equivalent magnetic noise density, EMND) vs. frequency for different ME structures.

Field sensing: Conclusions

- Generally, resonant bending modes were largely enhanced in the bidomain samples and almost suppressed in the unidomain ones both in the ME and impedance measurements;
- The PE coefficients of a LN crystal were found to be almost twice as large in a bidomain T-T structure produced by the DA method in comparison with a bidomain produced by SEH and a simple bimorph (due to elastic losses associated with the viscosity of the epoxy);
- A giant transversal ME effect of $1704 \text{ V}/(\text{cm}\cdot\text{Oe})$ at RT and $f = 6862 \text{ Hz}$ was obtained in a sample with a bidomain T-T $y+140^\circ$ -cut LN substrate fabricated by DA.

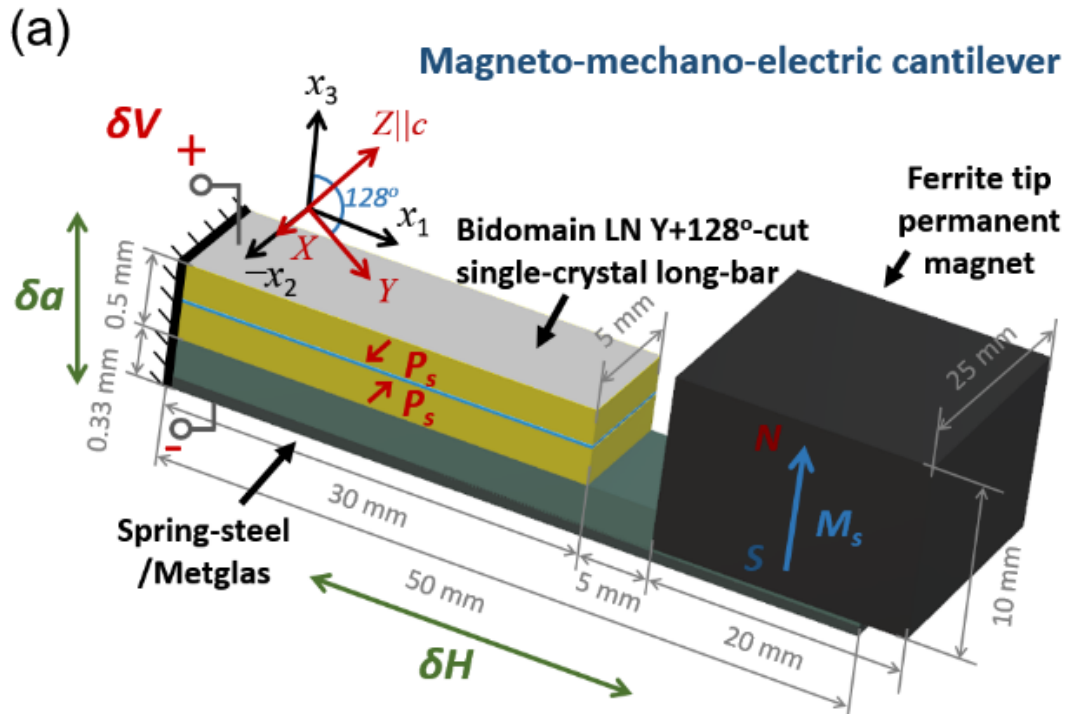
Field sensing: Conclusions

- Under ME resonant condition, the minimum detectable AC magnetic field with a signal-to-noise ratio of one was found to be as low as $92 \text{ fT}/\sqrt{\text{Hz}}$ at RT and a frequency of 6862 Hz;
- The use of a tuning fork-shaped ME structure permitted to increase the sensitivity to AC magnetic field by a factor of 6.7 at resonance and 7 to 25 times off resonance.
- In this study we have shown that lead-free bidomain LNO crystals could be useful, e.g., in the fabrication of thermally stable ME-based magnetic field sensors operating at low frequencies in the bending mode regime;
- Other advantages include: Low cost and simplicity of the materials and techniques, non-hysteretic PE response, low creep and ageing effects, entirely passive operation and ability to partially reject external vibrational and thermal noise.

Energy harvesting

With the recent thriving of low-power electronic microdevices and sensors, the development of components capable of scavenging environmental energy has become imperative. In this work, we studied bidomain LiNbO_3 (LN) single crystals combined with magnetic materials for dual, mechanical, and magnetic energy harvesting applications.

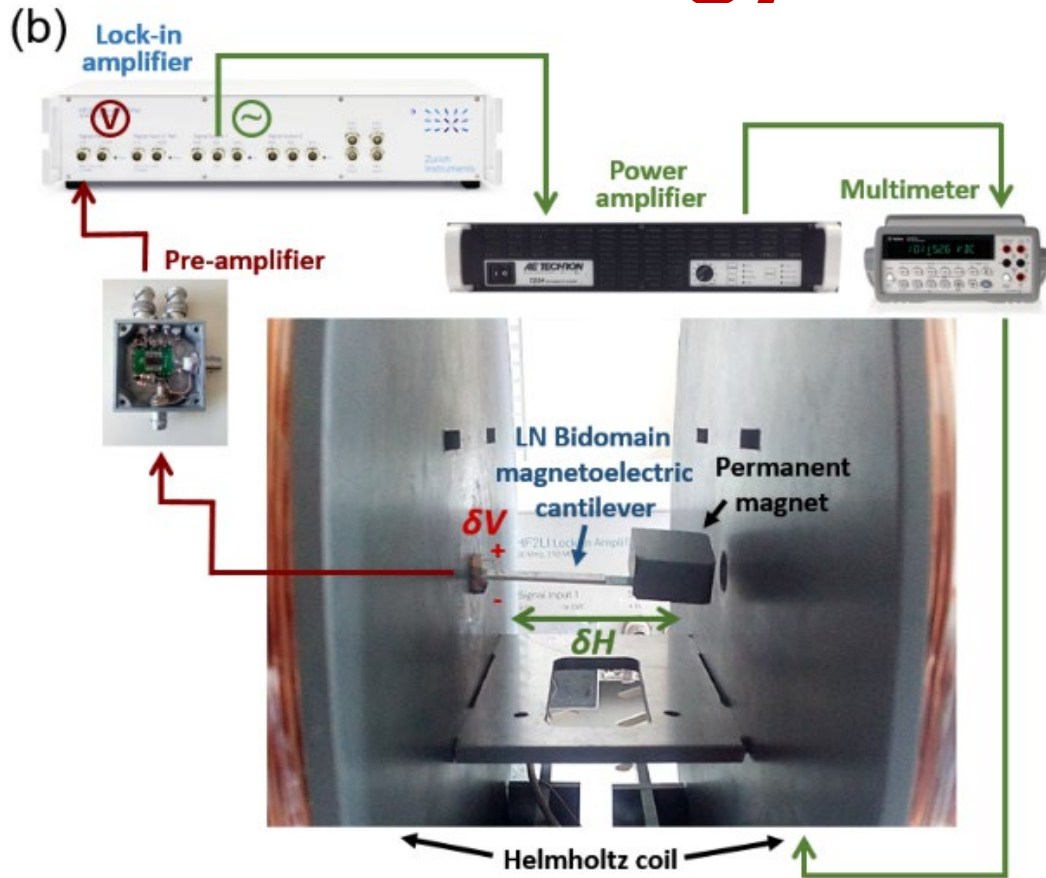
Energy harvesting



A “head-to-head” bidomain structure has been engineered in commercial LN $y+128^\circ$ -cut single-crystalline wafers using a DA technique. The asymmetric magneto-mechano-electric (MME) cantilever was prepared by bonding the long-bar bidomain LN to a sheet of spring steel, and this to a 29- μm -thick magnetostrictive metglas foil with the same length and width using a conductive silver epoxy.

A $20 \times 25 \times 10 \text{ mm}^3$ large tip hard ferrite permanent magnet ($\text{SrFe}_{12}\text{O}_{19}$) with a weight of 25 g, magnetized in the x_3 direction, was attached to the spring-steel layer, in order to further enhance its torque-induced magnetic response and decrease the resonance frequency.

Energy harvesting



Picture of the MME cantilever and scheme of the magnetic energy harvesting setup.

Vibration energy harvesting measurements were carried out on the MME cantilever with a vertical harmonic excitation of the base using a conventional setup composed of a shaker, accelerometer, preamplifier, and lock-in.

Energy harvesting

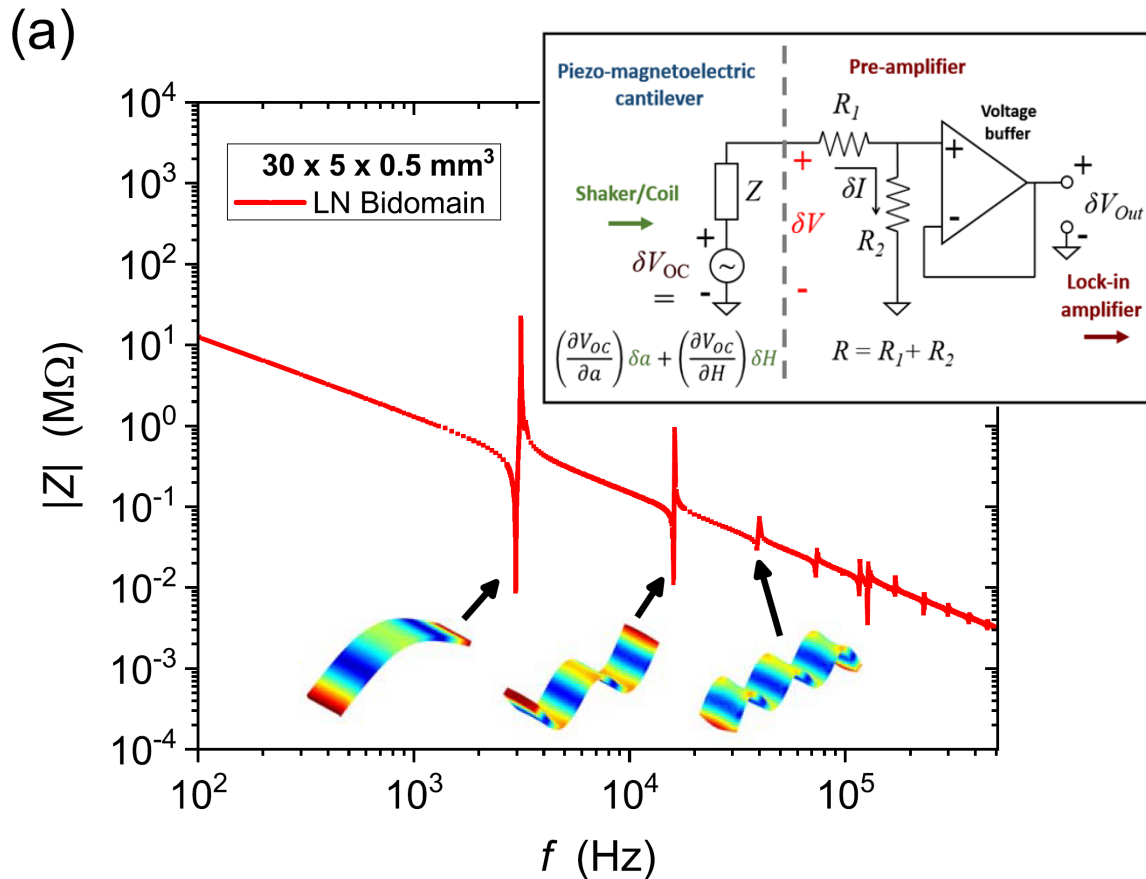
Even though it reduces the Q factor of the piezo crystal, the flexible spring-steel elastic layer was used with the intent of improving the mechanical reliability of the cantilever and increase its effective length and density, thus decreasing its fundamental resonance frequency.

Furthermore, a thickness ratio of the elastic to piezoelectric layer of ~ 0.4 should be able to sufficiently suppress the antiresonance impedance peak ($|Z|$) of the composite, thus increasing the maximum extractable power ($\langle P_{\max} \rangle \propto |\delta V_{oc}|^2 / (|Z| + Z')$).

A thin metglas layer was added in order to make use of its large permeability and magnetostriction to concentrate and convert applied magnetic fields into voltages through the elastically mediated ME effect.

The transversally magnetized tip permanent magnet was employed both as a tip mass and as a magnetic torque generator for an enhanced ME conversion ratio.

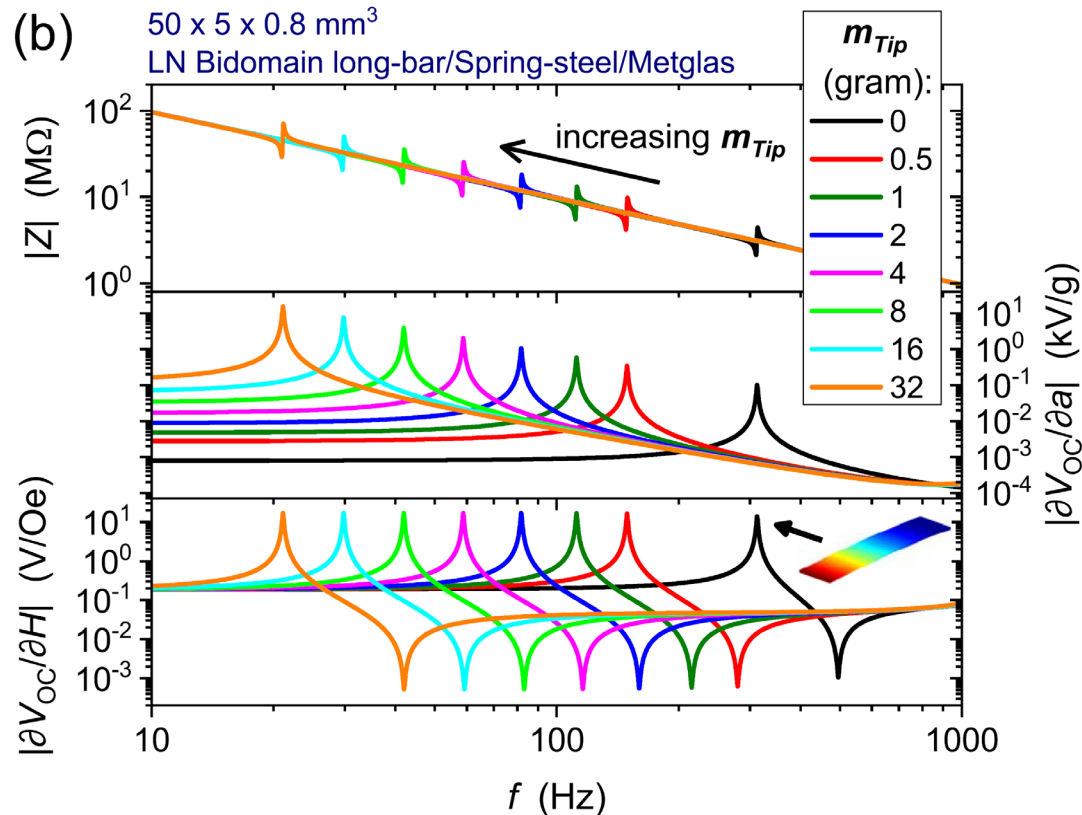
Energy harvesting



The impedance spectrum shows numerous resonance (minima) and antiresonance (maxima) peaks at relatively low frequencies which are associated with natural electromechanical bending modes.

Experimental impedance (Z) spectra of the $30 \times 5 \times 0.5 \text{ mm}^3$ bidomain LN crystal operating under free-bar conditions. Inset: the equivalent circuit of the MME composite and measurement unit. The first few natural EM bending mode shapes, obtained by an FEM simulation, are also represented.

Energy harvesting



Simulated results of the absolute impedance ($|Z|$), vibration open-circuit (OC) voltage-to-acceleration ratio ($|\partial V_{OC}/\partial a|$), and magnetic OC voltage-to-magnetic field ratio ($|\partial V_{OC}/\partial H|$) in an MME $50 \times 5 \times 0.8 \text{ mm}^3$ bidomain LN $y+128^\circ$ -cut / spring-steel / metglas cantilever with different proof tip masses (m_{Tip}).

Vibration energy harvesting

We were thus able to extract a maximum average power ratio of $\langle P_{\max} \rangle / |\delta a|^2 = 35.6 \text{ mW/g}^2$, with a matched resistance of $R = 40 \text{ M}\Omega$, corresponding to a power density of $6.9 \text{ mW}/(\text{cm}^3 \cdot \text{g}^2)$, taking into account the volume of the cantilever and tip proof mass, and a normalized volumetric power density of $0.24 \text{ }\mu\text{W}/(\text{mm}^3 \cdot \text{Hz} \cdot \text{g}^2)$.

However, the Q factor of this cantilever composite was found to be of only ca. 150, which is a result of the inferior Q factors of the spring-steel and metglas layers and a relatively large area of the interfaces bonded with viscous epoxy. For this reason, there should still exist **plenty of room for improvement** of the system.

Magnetic energy harvesting

The magnetic response revealed a resonant peak open-circuit voltage of 91 V/Oe and an average power of up to 50 $\mu\text{W}/\text{Oe}^2$, corresponding to a large magnetoelectric coefficient of 1.82 kV/(cm·Oe) and a power density of 9.7 $\mu\text{W}/(\text{cm}^3 \cdot \text{Oe}^2)$.

Summarizing, we developed a bidomain LN-based low-frequency, lead-free, and high-temperature MME system that in principle can scavenge power simultaneously from both low-level ambient vibration and magnetic field sources. With an appropriate storage circuit, it should thus be able to support ultralow-power electronic components. Due to its very large voltage transduction ratio, an attractive option could be a self-powered sensor used simultaneously as a vibration / magnetic sensor and a power generator when inactive.

Publications

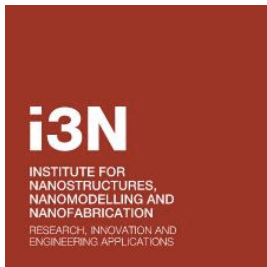
- J.V. Vidal, A.V. Turutin, I.V. Kubasov, A.M. Kislyuk, M.D. Malinkovich, Y.N. Parkhomenko, S.P. Kobeleva, N.A. Sobolev, A.L. Kholkin. “Dual vibration and magnetic energy harvesting with bidomain LiNbO₃ based composite”. IEEE Trans. Ultrasonics, Ferroelectrics, and Frequency Control, Vol. 67 (2020) 1219. <https://doi.org/10.1109/TUFFC.2020.2967842>
- A.V. Turutin, J.V. Vidal, I.V. Kubasov, A.M. Kislyuk, D.A. Kiselev, M.D. Malinkovich, Y.N. Parkhomenko, S.P. Kobeleva, A.L. Kholkin, and N.A. Sobolev. “Highly sensitive magnetic field sensor based on a metglas / bidomain lithium niobate composite shaped in form of a tuning fork”. J. Magn. Magn. Mater. Vol. 486 (2019) 165209. <https://doi.org/10.1016/j.jmmm.2019.04.061>
- J.V. Vidal, A.V. Turutin, I.V. Kubasov, A.M. Kislyuk, M.D. Malinkovich, Y.N. Parkhomenko, S.P. Kobeleva, O.V. Pakhomov, N.A. Sobolev and A.L. Kholkin. “Low-frequency vibration energy harvesting with bidomain LiNbO₃ single crystals”. IEEE Trans. Ultrasonics, Ferroelectrics, and Frequency Control, Vol. 66 (2019) 1480. <https://doi.org/10.1109/TUFFC.2019.2908396>
- I.V. Kubasov, A.M. Kislyuk, A.V. Turutin, A.S. Bykov, D.A. Kiselev, A.A. Temirov, R.N. Zhukov, N.A. Sobolev, M.D. Malinkovich, and Y.N. Parkhomenko. “Low-frequency Vibration Sensor with a Sub-nm Sensitivity Using a Bidomain Lithium Niobate Crystal”. Sensors, Vol. 19 (2019) 614. <https://doi.org/10.3390/s19030614>

Publications

- A.V. Turutin, I.V. Kubasov, A.M. Kislyuk, M.D. Malinkovich, S.P. Kobeleva, Yu.N. Parkhomenko, N.A. Sobolev. Utility model “Magnetolectric sensor of magnetic fields”. RU 188 677 U1. G01R 33/00 (2019.02). Priority from 08.02.2019. https://www.fips.ru/registers-doc-view/fips_servlet?DB=RUPM&DocNumber=188677&TypeFile=html
- A.V. Turutin, J.V. Vidal, I.V. Kubasov, A.M. Kislyuk, M.D. Malinkovich, Y.N. Parkhomenko, S.P. Kobeleva, O.V. Pakhomov, A.L. Kholkin, N.A. Sobolev. “Magnetolectric metglas/bidomain $y+140^\circ$ -cut lithium niobate composite for sensing fT magnetic fields”. Appl. Phys. Lett., Vol. 112 (2018) 262906. <https://doi.org/10.1063/1.5038014>
- A.V. Turutin, J.V. Vidal, I.V. Kubasov, A.M. Kislyuk, M.D. Malinkovich, Y.N. Parkhomenko, S.P. Kobeleva, A.L. Kholkin, N.A. Sobolev. „Low-frequency magnetic sensing by magnetolectric metglas/bidomain LiNbO₃ long bars“. J. Phys. D: Appl. Phys., Vol. 51 (2018) 214001. <https://doi.org/10.1088/1361-6463/aabda4>
- J.V. Vidal, A.V. Turutin, I.V. Kubasov, M.D. Malinkovich, Y.N. Parkhomenko, S.P. Kobeleva, A.L. Kholkin, N.A. Sobolev. „Equivalent magnetic noise in magnetolectric laminates comprising bidomain LiNbO₃ crystals“. IEEE Trans. Ultrasonics, Ferroelectrics, and Frequency Control, Vol. 64 (2017) 1102. <http://dx.doi.org/10.1109/TUFFFC.2017.2694342>

Publications

- J.V. Vidal, A.A. Timopheev, A.L. Kholkin, N.A. Sobolev, “Engineering the Magnetoelectric Response in Piezocrystal-Based Magnetoelectrics: Basic Theory, Choice of Materials, Model Calculations”. In: Nanostructures and Thin Films for Multifunctional Applications. Technology, Properties and Devices, ed. by I. Tiginyanu, P. Topala, V. Ursaki (Springer International Publishing, 2016) Chapter 6, pp. 189-226. ISBN 978-3-319-30197-6.
https://doi.org/10.1007/978-3-319-30198-3_6
- J.V. Vidal, A.A. Timopheev, A.L. Kholkin, N.A. Sobolev, “Dynamic Measurements of Magnetoelectricity in Metglas-Piezocrystal Laminates”. In: Nanostructures and Thin Films for Multifunctional Applications. Technology, Properties and Devices, ed. by I. Tiginyanu, P. Topala, V. Ursaki (Springer International Publishing, 2016) Chapter 7, pp. 227-265. ISBN 978-3-319-30197-6.
https://doi.org/10.1007/978-3-319-30198-3_7



UNIÃO EUROPEIA
Fundos Europeus Estruturais
e de Investimento

Thank you for your attention!



universidade de aveiro
theoria poiesis praxis